Reviewer 3.

We thank the reviewer for their careful reading of the manuscript. We address each of the comments in turn below, with the comments first given in bold, followed by the response in normal type, followed by any changes made to the manuscript.

While the title and main conclusions of the paper refer to wintertime haze events, the main modeling of the results summarized in Figure 8 appears to include both haze and non-haze events, while the brief discussion in section 4.3 separates the model analysis to haze and non-haze events, with Figure 14 showing the base model agreement worse under haze events. While the model appears to underestimate the measured RO2 concentration similarly for both events, the agreement of the predicted OH and HO2 concentrations with the measurements is better for the non-haze events. It appears from Figure 7 that the number of haze and non-haze events were roughly equal. As a result, it is not clear whether some of the main conclusions of the paper would be applicable to the haze events. It would be useful to illustrate in Figure 6, 8, and 13 how the different models in Table 1 are able to reproduce the radical measurements for haze and non-haze events. Is the estimation of the missing source different for the haze and non-haze events? Are the model results/conclusions different for the different events? While they may not be significant, any differences between the events should be discussed in more detail.

The reviewer makes a good point and we have now updated some figures to include separate comparisons for haze and non-haze events and introduced a more detailed discussion. In Figure 8 we do include diel profiles for both haze and non-haze events, and we have now updated Figure 14 to include modelling results from MCM-base, MCM-cHO2 as well as the measured values (including speciated RO_2 concentrations) for both haze and non-haze events, and we have included an additional discussion on the differences in model performance for the haze and non-haze periods for each of these species. The modified text is as follows:

"The measured complex RO_2 radical species peak at similar concentration inside (4.3 x 10^7 molecule cm^{-3}) and outside (4.6 x 10^7 molecule cm^{-3}) of haze. Unlike the complex RO_2, the simple RO_2 concentration peaks at a lower concentration inside of haze (3.4 x 10^7 molecule cm^{-3}) compared with outside (5.5 x 10^7 molecule cm^{-3}). The complex RO_2 is undepredicted by a factor of ~48 and ~12 inside and outside of haze, respectively. Whilst the simple RO_2 is undepredicted by a factor of ~66 and ~5.7 inside and outside of haze, respectively. The sharp increase for the underprediction of both simple and complex RO_2 inside of haze highlights the need of a large additional source of both simple and complex RO_2, especially under haze conditions. The increased contribution to kOH (s^{-1}) from VOCs from non-haze to haze conditions is a factor of: ~10 for aromatics, ~8 for alkenes and alkynes, ~6 for alkanes, ~9 for alcohols and ~2 for aldehydes. The large increase in relative contribution to kOH from aromatics, alkenes and alkynes is consistent with observation of higher complex RO_2 (compared to simple RO_2) during haze periods compared to non-haze periods. " and the updated Figure 14 is shown below:

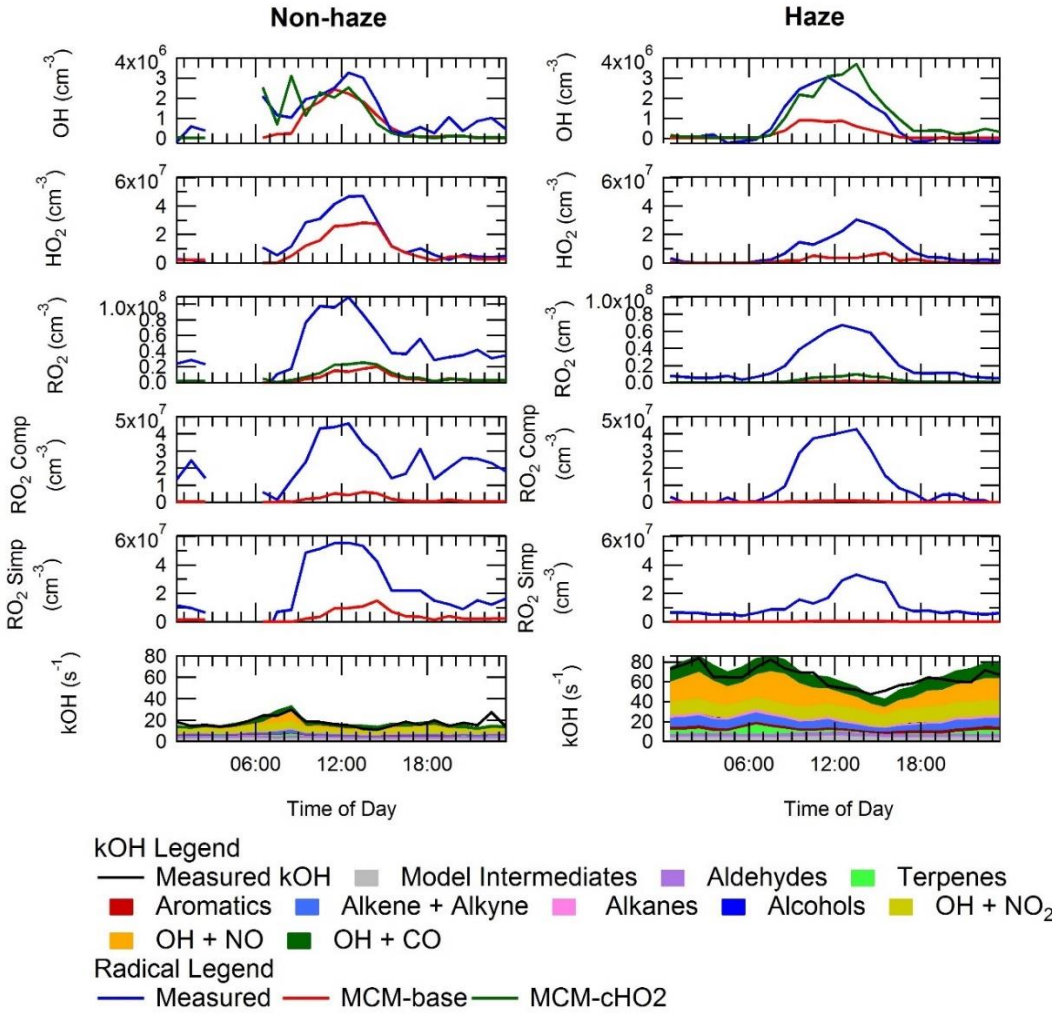

Figure 14. Average diel profiles for measured and modelled OH, HO_2, total RO_2, complex RO_2 (RO_2 comp), simple RO_2 (RO_2 simp) and kOH separated into haze (right) and non-haze (left) periods.

Figure 6, which shows the results of the photo-stationary state (PSS) expression for OH together with measurements of OH, has also been updated to include separation into haze and non-haze events. The PSS has been separated into haze and non-haze events and shows that during haze events the PSS captures the OH concentration, although the PSS does overpredict the OH concentration by ~1.35 between 09:30 – 14:30 in haze events. The overprediction by the PSS in haze events is highly influenced by the overprediction on the 04/12/2016. Whilst under non-haze conditions the PSS captures the OH concentration very well throughout the day. The production of from HONO increases in non-haze (~19%) compared with haze events (~7%). The updated text is as follows:

"The PSS has been separated into haze and non-haze events and shows that during haze events the PSS captures the OH concentration, although the PSS does overpredict the OH concentration by ~1.35 between 09:30 – 14:30 in haze events. However, the overprediction by the PSS in haze events is highly influenced by the overprediction on the 04/12/2016. Whilst under non-haze conditions the PSS captures the OH concentration very well throughout the day. The production of from HONO increases in non-haze (~19%) compared with haze events (~7%). " and the updated Figure 6 is shown below:

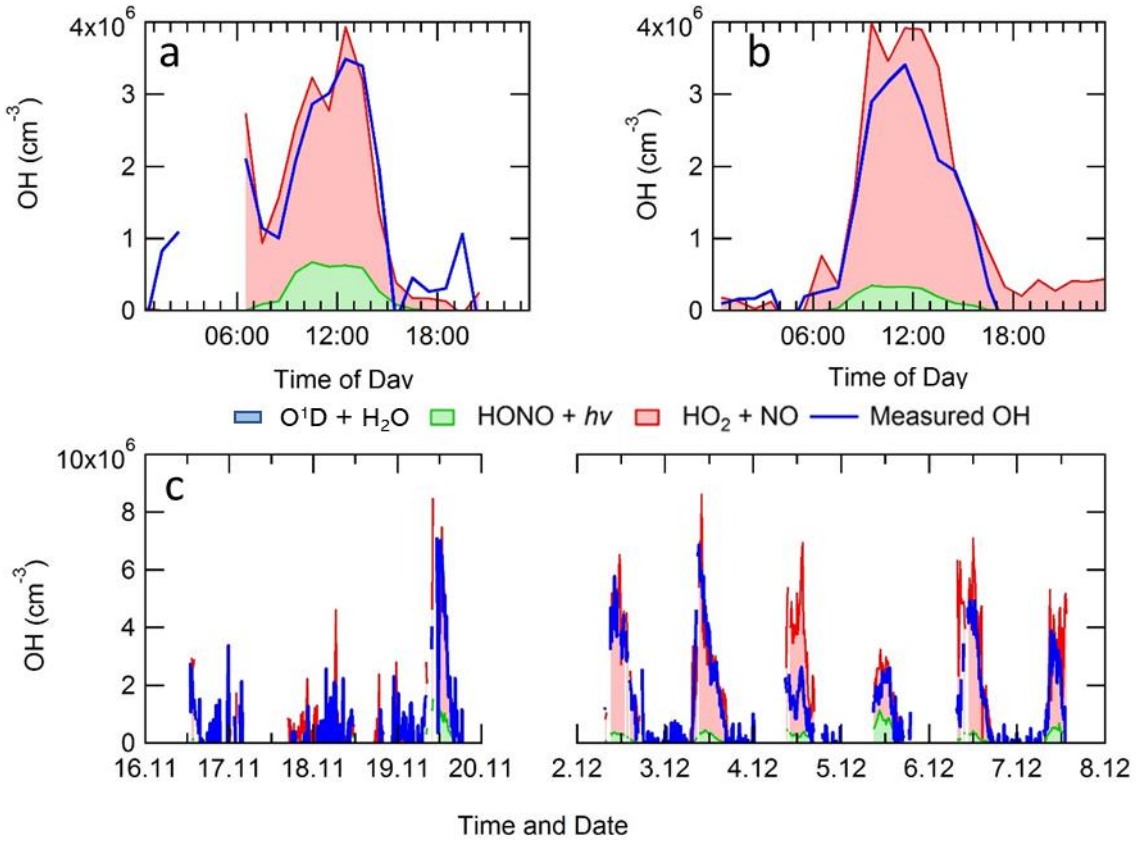

Figure 6. Average diel profile for observed and steady state calculated OH concentrations for: (a) non-haze, and(b) haze periods. Panel (c) shows a comparison time-series for the steady state calculation of OH and measured OH. The OH generated by O^1D+H_2O, although included in the key, is too small to be visible.

Figure 12 which shows the additional primary production required to bridge the gap between measured and modelled RO_2 and Figure 13 have been merged in an effort to shorten the manuscript. The merged graph (now Figure.12) has been separated into haze and non-haze events. The $P'RO_2$ is higher in the updated version of Figure 12 (see below) as the original Figure 12 had not been filtered for when measured data was available.

Figure 13 is now separated into haze and non-haze events too. A discussion has been added for the new graph.

Modified text :" The additional primary production of RO_x ($P'RO_x$) radicals required to bridge the gap between measured and modelled total RO_2 was found to peak at an average of 3.5 $x10^8$ molecule cm^{-3} s^{-1} at 08:30 non-haze events. Under haze conditions, the gap between measured and modelled total RO_2 was found to peak at an average of 4 x 10^8 molecule cm^{-3} s^{-1} at 13:30 as shown in Figure 12, calculated from Eq. 3 (Tan et al., 2018):

$$P'(RO_x) = k_{HO2+NO}\,[HO_2]\,[NO\ \ ] - P(HO_2)_{prim} - P(RO_2)_{prim} - k_{VOC}[OH] + L(HO_2)_{term} + L(RO_2)_{term} \quad \text{Eq. 3}$$

where $P(HO_2)_{prim}$, $P(RO_2)_{prim}$, $L(HO_2)_{term}$ and $L(RO_2)_{term}$ are the rates of primary production of HO_2, primary production of RO_2, termination of HO_2 and termination of RO_2, respectively. The overall (haze and non-haze) additional primary production peak of ~44 ppbv hr^{-1} (at 10:30) is almost nine times

larger than the additional RO_2 source that was required to resolve the measured and modelled RO_2 during the BEST-ONE campaign (5 ppbv h^{-1} during polluted periods, also calculated using Eq. 3), and is much larger compared to the known noon-average modelled primary production of RO_x during the APHH campaign of 1.7 ppbv hr^{-1}. The additional primary production required in non-haze rises sharply in the morning peaking at 08:30 (3.5 x 10^8 molecule cm^{-3}) and then decreases rapidly; whilst the additional source needed in haze events peaks at 4 x 10^8 molecule cm^{-3} s^{-1}. The additional primary source required during haze events through-out the day is ~7 times higher than that during non-haze events."

Modified text: "However, the MCM-PRO2 run overpredicts the observed HO_2 during haze and non-haze events by a factor of 3.4 and 2.5, respectively, with the large overprediction of HO_2 in haze and non-haze events driving the overprediction of OH by a factor of 2.2 and 2.5. This highlights that the additional primary RO_2 source may be an RO_2 species that does not readily propagate to HO_2, this has also been discussed in Whalley et al. (2020). "

Modified text: "The comparison of MCM-PRO2-SA with both measurements and MCM-PRO2 (see Table 2 for details) is shown in Figure 12 and shows that the uptake of HO_2 only has a small impact <6% and <14% on the modelled levels of OH, HO_2 and RO_2 during haze and non-haze events, respectively."

Updated Figure 13.

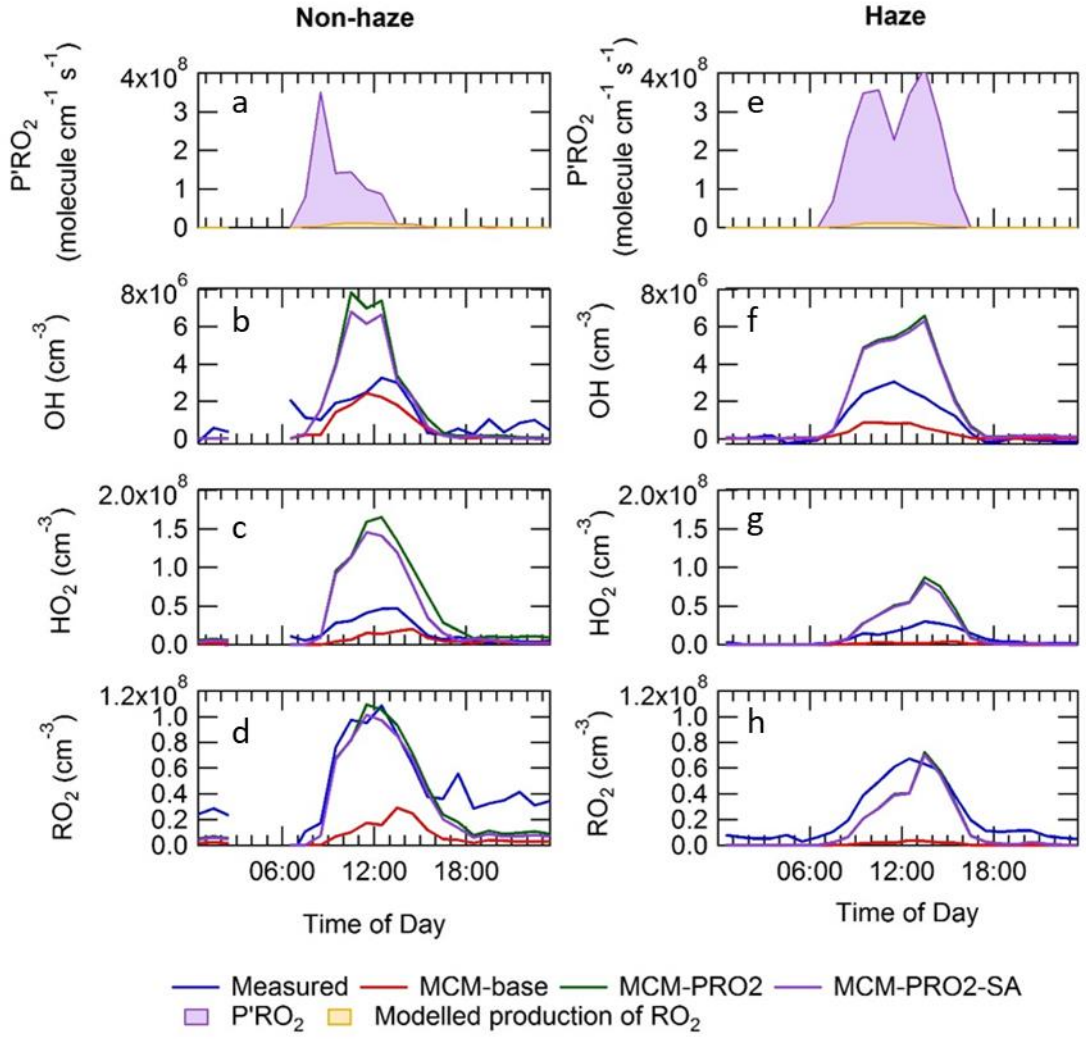

Figure 13. Average diel comparison of measurements of P'RO_2, OH, HO_2 and sum of RO_2 with the MCM-base, MCM-PRO2 and MCM-PRO2-SA box-model runs inside (e – h) and outside (a – d) of haze events. The average diel is from the entire APHH winter campaign. See text and Table 2 for definitions of each of the model runs.

Lisa K Whalley, Eloise J Slater, Robert Woodward-Massey, Chunxiang Ye, James D Lee, Freya Squires, James R Hopkins, Rachel E Dunmore, Marvin Shaw, Jacqueline F Hamilton, Alastair C Lewis, Archit Mehra, Stephen D Worrall, Asan Bacak, Thomas J Bannan, Hugh Coe, Bin Ouyang, Roderic L Jones, Leigh R Crilley, Louisa J Kramer, William J Bloss, Tuan Vu, Simone Kotthaus, Sue Grimmond, Yele Sun, Weiqi Xu, Siyao Yue, Lujie Ren, W. Joe F Acton, C. Nicholas Hewitt, Xinming Wang, Pingqing Fu, and Dwayne E Heard : Evaluating the sensitivity of radical chemistry and ozone formation to ambient VOCs and NOx in Beijing, *Atmos. Chem. Phys Disc*, 2020.

2) The authors should clarify their definition of OHwave and OHchem on pages 6-7. The current description suggests that OHchem is the on-line background measurement including interferences, while OHwave is the off-line background measurement. However, Figure 3 compares the measured OH concentration determined using chemical modulation (signal – OHchem background) with that determined by spectral modulation (signal – OHwave background), not a comparison of the background signal measured by both methods.

The definition of OHwave and OHchem and the discussion surrounding Figure 3 has been tightened up in the paper, and the modified sections of text are as follows:

Modified text

"OHchem is the online OH signal – OHchem background and OHwave is the OH online signal – Ohwave background."

3) Related to this, the authors state that the spectral modulation measurements were also corrected for laser-generated OH from ozone photolysis + H2O (page 7). Based on the Woodward-Massey et al. (2020) paper, it appears that the interference was calculated based on laboratory measurements of the interference as a function of ozone, water and laser power. This should be clarified. Since this interference would be measured by chemical modulation, a comparison of the measured interference with that calculated would provide additional confidence in the OHChem measurement as well as the accuracy of the interference estimate.

OHwave data were indeed corrected for the known interference from O_3 + H_2O, with further details available from Woodward-Massey et al. (2020). The O_3 + H_2O interference calculated was very small (median ~8.5 x 10^3 molecule cm^{-3}) due to the low concentrations of H_2O and O_3.

Modified text: " OHwave data were corrected for the known interference from O_3 + H_2O, see Woodward-Massey et al. (2020) for further details. The O_3 + H_2O interference calculated was very small (median ~8.5 x 10^3 molecule cm^{-3}) due to the low concentration of H_2O and O_3. All figures and calculation from now on have used OHwave as it is the most extensive time-series (12 days compared to 5 days)."

Woodward-Massey, R., Slater, E. J., Alen, J., Ingham, T., Cryer, D. R., Stimpson, L. M., Ye, C., Seakins, P. W., Whalley, L. K., and Heard, D. E.: Implementation of a chemical background method for atmospheric OH measurements by laser-induced fluorescence: characterisation and observations from the UK and China, Atmos. Meas. Tech., 13, 3119–3146, https://doi.org/10.5194/amt-13-3119-2020, 2020.

4) There is little discussion of the HO2, HO2*, and RO2 experimental measurement conditions, except that it appears that the conditions were similar to that in the ClearfLo study. The paper would

benefit from a brief discussion of the experimental conditions employed in this study. It appears that only a single NO flow was used in the HOx detection cell for these measurements, in contrast to the use of two NO flows used to measure HO2 and HO2* (RO2i) during ClearfLo (Whalley et al., 2018). Instead it appears that HO2* was measured using the ROxLIF detection cell. While it is stated that the ROxLIF method is described "in detail below" (page 5), the paper again references Whalley et al. (2018) instead of providing details. Given the high concentrations of NOx in this study, how did the authors account for potential interferences from the decomposition of HO2NO2 and CH3O2NO2? More details on the experimental measurements are needed. In addition the authors should clarify how the simple RO2 and complex RO2 were derived from the measurements. It appears that complex RO2 was obtained from the difference between the HO2* ROxLIF measurements and the FAGE HO2 measurements, while the simple RO2 were obtained from the difference between the ROxLIF RO2 and HO2*measurements. Much of this information could go into the Supplement.

- Description of the RO_xLIF instrument and the running conditions has been added to the paper. The text is as follows:

"The ROxLIF flow reactor (83 cm in length, 6.4 cm in diameter) was coupled to the second FAGE detection cell to allow for detection of RO_2 (total, complex and simple) using the method outlined by Fuchs et al. (2008). The flow reactor was held at ~30 Torr and drew ~7.5 SLM through a 1 mm pinhole ID (in-diameter). The flow reactor was operated in two mode: in the first (HO_x mode) 125 sccm of CO (Messer, 10% in N_2) was mixed with ambient air close to the pinhole to convert OH to HO_2. In the second (RO_x mode), 25 sccm of NO in N_2 (Messer, 500 ppmv) was also added to the CO flow to convert RO_2 into OH. The CO present during RO_x mode rapidly converts the OH formed into HO_2. The air from the RO_xLIF flow reactor was drawn (5 SLM) into the FAGE fluorescence cell (held at ~1.5 Torr) and NO (Messer, 99.9%) was injected into the fluorescence cell to convert HO_2 to OH. In HO_x mode a measure of OH + HO_2 + cRO_2 was obtained; whilst RO_x measured OH + HO_2 + ΣRO_2. sRO_2 concentration was determined by subtracting the concentration of cRO_2, HO_2 and OH from RO_x.

In previous laboratory experiments the sensitivity of the instrument to a range of different RO_2 was investigated and can be found in Whalley et al.(2018). Similar sensitivities were determined for a range of RO_2 species that were tested and agreed well with model-determined sensitivities. For comparison of the modelled RO_2 to the observed RO_2-total, RO_2-complex and RO_2-simple, the RO_xLIF instrument sensitivity towards each RO_2 species in the model was determined by running a model first under the RO_xLIF reactor and then the RO_xLIF FAGE cell conditions (NO concentrations and residence times) to determine the conversion efficiency of each modelled RO_2 species to HO_2. "- The values of RO_2 (simple, complex and total) in the paper have not been corrected for the decomposition of HO_2NO_2 and $CH_3O_2NO_2$ but an estimation has been added to the supplementary material and shows the correction from the decomposition of HO_2NO_2 and $CH_3O_2NO_2$ is ~6 %, ~8 % and 4 % for total, complex and simple RO_2, respectively.

Signposting text has been added in the main paper to the supplementary material discussion for HO_2NO_2 and $CH_3O_2NO_2$ decomposition. Modified text: "The potential interference in the RO_2 measurements from HO_2NO_2 and $CH_3O_2NO_2$ has been explored in the supplementary material in section S1.4, however the data presented through-out the paper are the uncorrected data since the correction is small (correction from the decomposition of HO_2NO_2 and $CH_3O_2NO_2$ is ~6 %, ~8 % and 4 % for total, complex and simple RO_2, respectively.)"

Information added to the supplementary material:

"**S1.4 Estimating the contribution of HO_2NO_2 and $CH_3O_2NO_2$ to the RO_2 signal**

In the main paper we do not apply a correction for a possible contribution of pernitric acid (PNA, HO_2NO_2) and methyl peroxy nitric acid (MPNA, $CH_3O_2NO_2$). The MPNA decomposition will contribute

to the simple RO_2 and total RO_2 whilst the PNA contributes to the complex and total RO_2 measurements. The concentration of HO_2NO_2 and $CH_3O_2NO_2$ was modelled using the MCM-base model, then in agreement with the work by Fuchs et al.(2008) 0.43 % and 9 % of the HO_2NO_2 and $CH_3O_2NO_2$ is calculated to decompose and contribute to the RO_2 signal. The rate of decomposition in the Julich and Leeds RO_xLIF reactors is expected since the design and residence time (~1 second) are similar. The comparison of the measured total, simple and complex RO_2 with the corrected values is shown in Figure S5. Figure S5 shows that the correction from the decomposition of HO_2NO_2 and $CH_3O_2NO_2$ is ~6 %, ~8 % and 4 % for total, complex and simple RO_2, respectively.

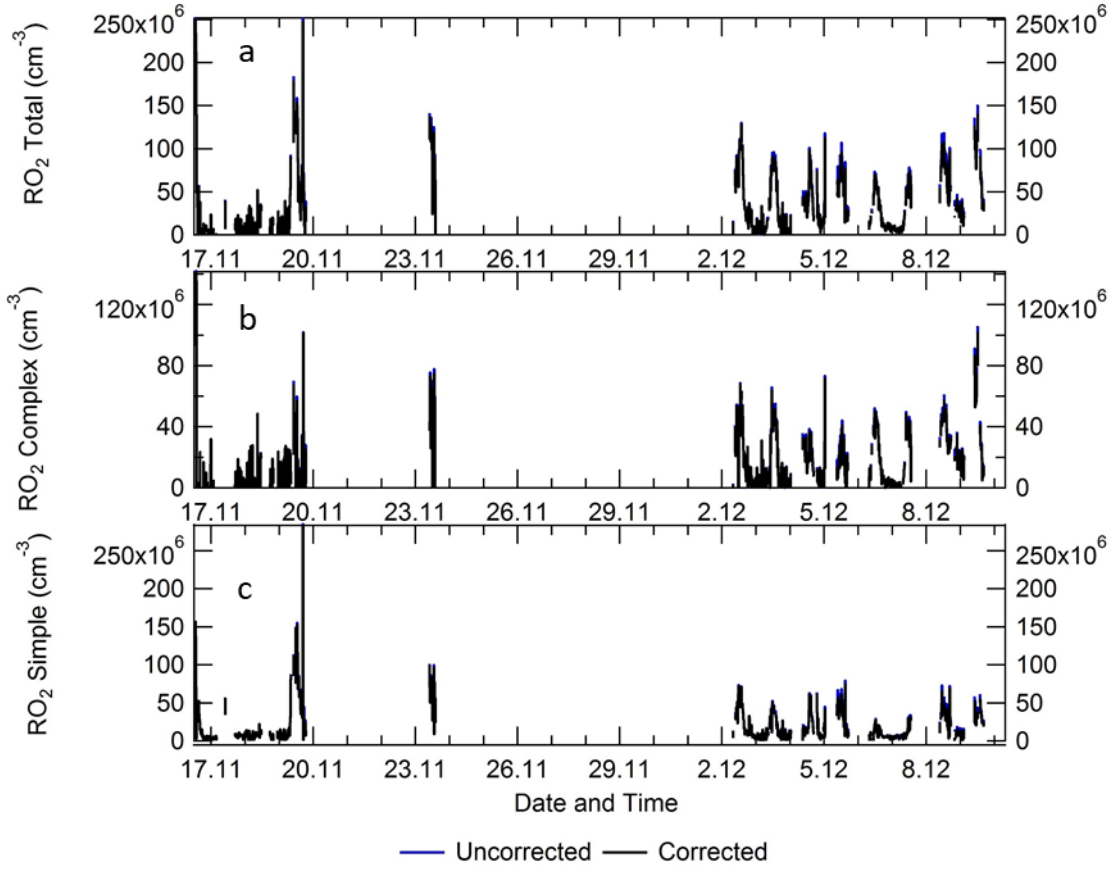

Figure S5 a) Timeseries comparison for measured total RO_2 (blue) and total RO_2 corrected (black) for the decomposition from HO_2NO_2 and $CH_3O_2NO_2$. b) Timeseries comparison for measured complex RO_2 (blue) and complex RO_2 corrected (black) for the decomposition from HO_2NO_2. c) Timeseries comparison for measured simple RO_2 (blue) and simple RO_2 corrected (black) for the decomposition from $CH_3O_2NO_2$.

“

Fuchs, H., Holland, F. and Hofzumahaus, A., 2008. Measurement of tropospheric RO_2 and HO_2 radicals by a laser-induced fluorescence instrument. *Review of Scientific Instruments*, *79*(8), p.084104.

Whalley, L. K., Stone, D., Dunmore, R., Hamilton, J., Hopkins, J. R., Lee, J. D., Lewis, A. C., Williams, P., Kleffmann, J., and Laufs, S.: Understanding in situ ozone production in the summertime through radical observations and modelling studies during the Clean air for London project (ClearfLo), Atmospheric Chemistry and Physics, 18, 2547-2571, 2018.

5) Similarly, there is no discussion of the experimental method used to measure total OH reactivity. From the information given in Figure 7, it appeared that the OH reactivity was calculated based on

the measured OH sinks, but it is clear from Figure 8 that total OH reactivity was measured. Is the measured OH reactivity shown in Figure 7?

Measured OH reactivity is shown in Figure 7 and represented by the black line, and the caption has been updated to make this clear:

Updated Figure 7. caption :" Time-series of OH, b) HO_2, c) total RO_2, d) partly-speciated RO_2 and e) Measured (black) and modelled (stacked plot) OH Reactivity. For (a)-(c), the raw measurements (6-min data acquisition cycle) are blue open circles with 15 min average represented by the solid blue line. The 15 min model output in a-c is represented by the red line for OH, HO_2 and RO_2. The partly-speciated RO_2 is separated into simple (gold open circles) and complex (purple open circles). The individual contributions of the model to the OH reactivity is given below the graph. The grey shaded areas show the haze periods when $PM_{2.5}$ > 75 μg m^{-3}."

A section has also been added describing the OH reactivity method, modified text is shown below copied from response to reviewer 2: "OH reactivity measurements were made using the laser flash photolysis pump-probe technique and the instrument is described in detail in Stone et al. (2016). Ambient air was drawn into the reaction cell (85 cm in length, 5 cm in diameter) at 12 SLM. Humidified ultra-high purity air (Messer, Air Grade Zero 2) passed a low-pressure Hg lamp at 0.5 SLM to generated ~ 50 ppbv of O_3 which was mixed with the ambient air. The O_3 was photolyzed at 266 nm to generate a uniform OH concentration across the reaction cell. The change in the OH radical concentration from pseudo-first-order loss with species present in ambient air was monitored by sampling the air from the reaction cell into a FAGE detection cell at ~1.5 Torr. The 308 nm probe laser (same as the FAGE laser describe above) was passed across the gas flow in the FAGE cell to excite OH radicals, and then detected the fluorescence signal at ~ 308 nm detected by a gated channel photomultiplier tube. The OH decay profile owing to reactions with species in ambient air was detected in real time. The decay profile was averaged for 5-mins and fitted with a first-order rate equation to find the rate coefficient describing the loss of OH (k_{loss}), with k_{OH} determined by subtracting the physical loss of OH (k_{phys}). The OH reactivity data were fitted with a mono-exponentially decaying function as no bi-exponential behaviour was observed, even at the highest NO concentrations, and hence there is no evidence for recycling from HO_2 + NO impacting on the retrieved values The total uncertainty in the ambient measurements of OH reactivity is ~ 6% (Stone et al. 2016). "

Stone, D., Whalley, L.K., Ingham, T., Edwards, P., Cryer, D.R., Brumby, C.A., Seakins, P.W. and Heard, D.E., 2016. Measurement of OH reactivity by laser flash photolysis coupled with laser-induced fluorescence spectroscopy. *Atmospheric Measurement Techniques*, pp.2827-2844.

brief description of the measurement technique should be included. Given the high mixing ratios of NO that were observed, did interference from the HO2+NO reaction impact the OH reactivity measurements?

The kOH decays show no biexponential behaviour suggesting that recycling from HO_2 + NO was not observed and all decays were fitted with a single exponential decay. Details of the OH reactivity instrument have been added to the instrumental details section, and relevant citations are given. The total uncertainty in the ambient measurements of OH reactivity is ~ 6% (Stone et al. 2016). The new text describing the method is as follows:

"OH reactivity measurements were made using the laser flash photolysis pump-probe technique and the instrument is described in detail in Stone et al. (2016). Ambient air was drawn into the reaction cell (85 cm in length, 5 cm in diameter) at 12 SLM. Humidified ultra-high purity air (Messer, Air Grade Zero 2) passed a low-pressure Hg lamp at 0.5 SLM to generated ~ 50 ppbv of O_3 which was mixed with the ambient air. The O_3 was photolyzed at 266 nm to generate a uniform OH concentration across the reaction cell. The change in the OH radical concentration from pseudo-first-order loss with species present in ambient air was monitored by sampling the air from the reaction cell into a FAGE detection

cell at ~1.5 Torr. The 308 nm probe laser (same as the FAGE laser describe above) was passed across the gas flow in the FAGE cell to excite OH radicals, and then detected the fluorescence signal at ~ 308 nm detected by a gated channel photomultiplier tube. The OH decay profile owing to reactions with species in ambient air was detected in real time. The decay profile was averaged for 5-mins and fitted with a first-order rate equation to find the rate coefficient describing the loss of OH (k_{loss}), with k_{OH} determined by subtracting the physical loss of OH (k_{phys}). The OH reactivity data were fitted with a mono-exponentially decaying function as no bi-exponential behaviour was observed, even at the highest NO concentrations, and hence there is no evidence for recycling from HO_2 + NO impacting on the retrieved values The total uncertainty in the ambient measurements of OH reactivity is ~ 6% (Stone et al. 2016). ."

Abstract: There have been previous measurements of radicals at similar NO levels in Mexico City (Shirley et al., ACP, 2006; Dusanter et al., ACP, 2009).

We thank for the reviewer for pointing this out. The abstract has been corrected as follows:

"Wintertime *in situ* measurements of OH, HO_2 and RO_2 radicals and OH reactivity were made in central Beijing during November and December 2016. Exceptionally elevated NO was observed on occasions, up to ~250 ppbv."

The caption in Figure 3 states that the gray points represent an acquisition cycle of 6 min, but the legend states that they are 4 min averages.

The average stated in the legend is for the OH measurement period only, while the overall data acquisition is for the whole measurement period (including 2 minutes of HO_2 measurements).

The caption has been updated, and now reads as follows:

"Overall intercomparison of OHwave and OHchem observations from the winter 2016 APHH campaign. Grey markers represent raw data (6 min acquisition cycle, 4 minutes and 2 minutes for the OH and HO_2 measurements), with 1 h averages (±2 standard error, SE) in red. The thick red line is the orthogonal distance regression (ODR) fit to the hourly data, with its 95% confidence interval (CI) bands given by the thin red lines; fit errors given at the 2σ level. For comparison, 1:1 agreement is denoted by the blue dashed line. OHwave data were corrected for the known interference from $O_3 + H_2O$. Taken from (Woodward-Massey et al., 2020) where further details can be found."

While the VOC measurements used to constrain their model are given in Table 1, the paper would benefit from additional information on the instruments used to measure the other model constraints. Even though this information may be provided in a separate campaign paper, a table similar to that in Whalley et al. (2018) could be included in the Supplement.

This has been covered in response to reviewer 2, and the response to reviewer 2 is copied below:

We have added a Table (Table 2) which describes the methods used for some of the key species which are used to constrain the model. For many of the other species used to constrain the model, details are given in Shi et al 2018, and we have made a clear reference to that paper.

Modified wording "The accuracy and precision of trace gas species can be found in Table 2, details on the HONO measurements used in the modelling scenarios can be found in Crilley et al.(2019). Details for other measurements can be found in Shi et al.(2018)"

The following table has been added to the manuscript:

Instrument	Technique	2σ Uncertainty / %	2σ Precision/ ppbv
O_3, TEi49i	UV absorption	4.04	0.28[1]
NO, TEi42i-TL	Chemiluminescence via reaction with O_3	4.58	0.03[1]
SO_2, TEi43i	UV fluorescence	3.12	0.03[1]
NO_2, CAPS, T500U	Cavity enhanced absorption spectroscopy	5.72	0.04[1]
HONO	LOPAP x2, BBCEAS x 2, ToF-CIMS and SIFT-MS	9 – 22%	0.025 – 0.130

Table 2. Instruments and techniques used to measure key model constraints. 2σ uncertainties for the measured trace gas species used in the modelling scenarios are quoted. [1]Precision is given for 15-minute averaging time. For details of the HONO measurements please see Crilley et al.(2019).

It appears from Figure 4 that HONO measurements were not available between 2/12 and 5/12, but the steady-state calculations shown in Figure 6 include data between 2/12-8/12 and were chosen "as full data coverage for HONO, NO, j values, radical and k(OH) measurements were available." Was HONO available on all these days?

This has been covered in response to reviewer 1, the response to reviewer 1 is copied below:

The HONO dataset shown in Figure 4 was from one HONO instrument only and the HONO used in the steady-state calculation was the HONO recommended by Crilley et al. (2019) based on measurements by several instruments during the campaign, and represents a more complete dataset. The HONO shown in Figure 4 has now been updated to those recommended by Crilley et al. (2019), and are the values that have been used in the steady-state calculation and MCM model. Low NO_x would lead to reduction in recycling from HO_2 + NO, which is the largest source of OH production, and hence on 5/12 at the lowest NOx, this makes HONO the largest contributor to the rate of OH production. Figure 4 has been updated with the correct HONO dataset, see response above for the updated version of Figure 4 along with the updated caption.

Crilley, L. R., Kramer, L. J., Ouyang, B., Duan, J., Zhang, W., Tong, S., Ge, M., Tang, K., Qin, M., Xie, P., Shaw, M. D., Lewis, A. C., Mehra, A., Bannan, T. J., Worrall, S. D., Priestley, M., Bacak, A., Coe, H., Allan, J., Percival, C. J., Popoola, O. A. M., Jones, R. L., and Bloss, W. J.: Intercomparison of nitrous acid (HONO) measurement techniques in a megacity (Beijing), Atmos. Meas. Tech., 12, 6449–6463, https://doi.org/10.5194/amt-12-6449-2019, 2019.

See updated figure and caption below:

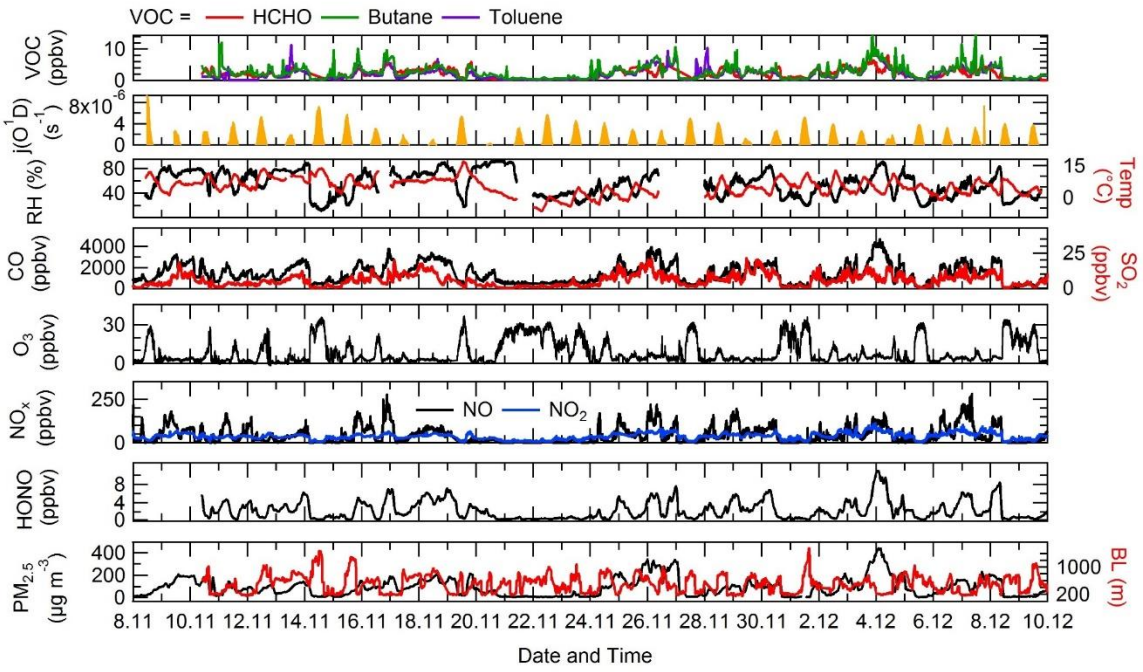

Figure 4. Time-series of $j(O^1D)$, relative humidity (RH), temperature (Temp), CO, SO_2, O_3, NO_x, HONO, boundary layer (BL), $PM_{2.5}$, HCHO, butane and toluene from the 8th of November to 10th December 2016 at Institute of Atmospheric Physics (IAP), Beijing.

Page 16 and Table 4: The text and table state that the average OH maximum was 2.7 E6 cm-3, but a value of 3.03 E6 cm-3 is stated on page 18.

We apologise for the inconsistency. The correct value is 2.7 x 10^6 molecule cm^{-3}, and this has been corrected on page 18.

Page 19: I am not sure late February/March would be considered mid-summer in Boulder, but rather late winter/early spring.

Indeed, that is true. We have used the words 'closer to spring' instead.

Figure 9: The authors should clarify whether this is an experimental radical budget or one derived from the model.

The caption now explicitly states that the radical budget is calculated from the model.

New caption for Figure 9. "Rates of primary production (top panel) and termination (bottom panel) for RO_x radicals (defined as OH + HO_2 + RO + RO_2) calculated for MCM-base model separated into haze (right) and non-haze (left) periods. The definition of haze is when $PM_{2.5}$ exceeds 75 μm^{-3}. The production from: $O^1D + H_2O$, VOC + NO_3, carbonyls + *hv* and the termination reactions: $RO_2 + HO_2$, $HO_2 + HO_2$, $HO_2 + NO_2$, although shown in the key, are not visible and contributed <1% of the total prodcution and termination."

Given the importance of HONO to radical initiation, how sensitive was the model to the systematic differences in the HONO measurements as described in Crilley et al. (2019)?

Rather than show the impact of different HONO concentrations using the MCM model, we have demonstrated the impact of different HONO measurements using a sensitivity analysis of the PSS calculation for OH. The model was not used since the effect would be small as the underprediction of the radicals derives from the RO_2 chemistry which does not lead to any terms in the PSS equation. The sensitivity of the results of the PSS calculation towards the HONO concentration has been included in

the supplementary material, and shows the PSS can be perturbed up to 17% when the HONO measurement is increased/decreased by 40%.

Some new text has been added to the supplementary material as follows:

"**S1.5 Exploring the sensitivity of the photostationary steady-state OH calculation to the HONO concentration.**

The HONO concentration used to constrained both the model and the photostationary steady-state calculation was the suggested value by Crilley et al.(2019). During the campaign there was several HONO measurement present and, although the measurements agreed on temporal trends and variability (r^2>0.97), the absolute concentration diverged between 12 – 39%, the value suggested by Crilley et al. (2019) was the mean of the measurements. Since HONO is a primary source of OH the impact of the variable HONO concentration has been explored by increasing and decreasing the HONO by 40%, the results are shown in Figure S6. Figure S6 shows that the variation observed in the HONO measurements can increase/decrease the PSS up to 17% which is smaller than the error on the measured OH of ~26%.

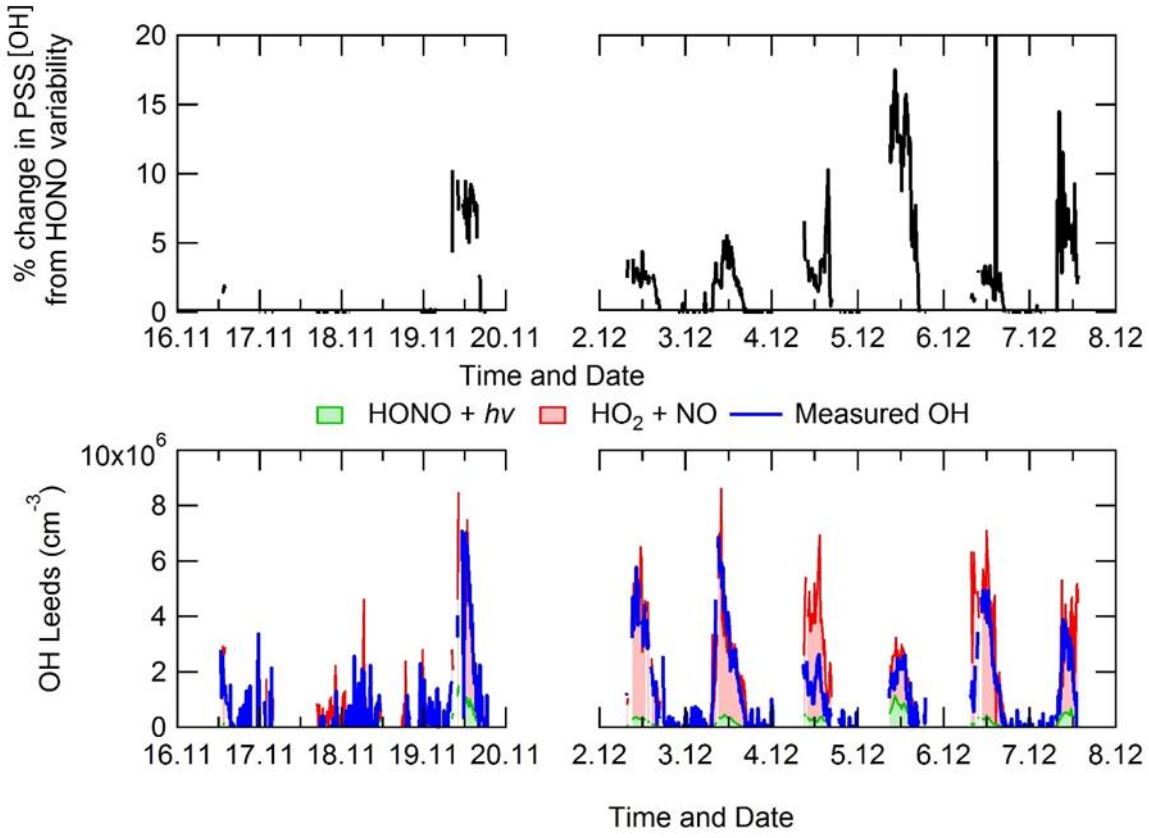

Figure S6 Top – Percentage change in the OH calculated from the PSS when the HONO is varied by 40%. Bottom – Comparison of the measured OH and the OH calculated from the PSS using the mean suggested value by Crilley et al. (2019).

"

and a sentence has been added to the main paper regarding the conclusions of this sensitivity analysis, as follows:

"The different HONO measurements present during the APHH campaign varied up-to ~40%, the sensitivity of the PSS on measured HONO is shown in the supplementary material section S1.5."

Page 26: There appears to be a problem with the signs in Equation 3 (see the corresponding equation in Tan et al. (2018))

This has now been fixed.

Page 26, line 560: Here it is stated that the P'(ROx) is 1.2 E8 cm-3 s-1, but on page 27 line 575 states that it is 1.01 E8 cm-3 s-1.

We apologise for the inconsistency. The $P'RO_2$ is higher in the updated version of Figure 12 (see above) as the original Figure 12 had not been filtered for when measured data was available only.

The correct value is 3×10^8 cm^{-3} s^{-1} and has been corrected in both instances.